NJC

Accepted Manuscript

This is an *Accepted Manuscript*, which has been through the Royal Society of Chemistry peer review process and has been accepted for publication.

Accepted Manuscripts are published online shortly after acceptance, before technical editing, formatting and proof reading. Using this free service, authors can make their results available to the community, in citable form, before we publish the edited article. We will replace this *Accepted Manuscript* with the edited and formatted *Advance Article* as soon as it is available.

You can find more information about *Accepted Manuscripts* in the Information for Authors.

Please note that technical editing may introduce minor changes to the text and/or graphics, which may alter content. The journal's standard Terms & Conditions and the Ethical guidelines still apply. In no event shall the Royal Society of Chemistry be held responsible for any errors or omissions in this *Accepted Manuscript* or any consequences arising from the use of any information it contains.

ROYAL SOCIETY OF CHEMISTRY

www.rsc.org/njc

Table of content only

_N_-Heterocyclic Carbene Rhodium(I) Complexes Containing an Axis of Chirality: Dynamics and Catalysis

Maria Cristina Cassani, Marta Anna Brucka, Cristina Femoni, Michele Mancinelli, Andrea Mazzanti, Rita Mazzoni,* Gavino Solinas*

Dipartimento di Chimica Industriale "Toso-Montanari", viale Risorgimento 4, I-40136 Bologna, Italy.

Novel rhodium(I) complexes [RhCl(NBD)(NHC)] [NHC = 1-benzyl-3-R-imidazolin-2-ylidene; R = Me, Bz, Tr, ^{t}Bu]: determination of the rotation barriers about the Rh-carbene and catalytic activity in the hydrosilylation of terminal alkynes.

*To whom correspondence should be addressed. E-mail: maria.cassani@unibo.it (M.C.C.), rita.mazzoni@unibo.it (R.M.); fax: +39 0512093694; phone: +39 051 2093700.

Graphic for Table of Content only

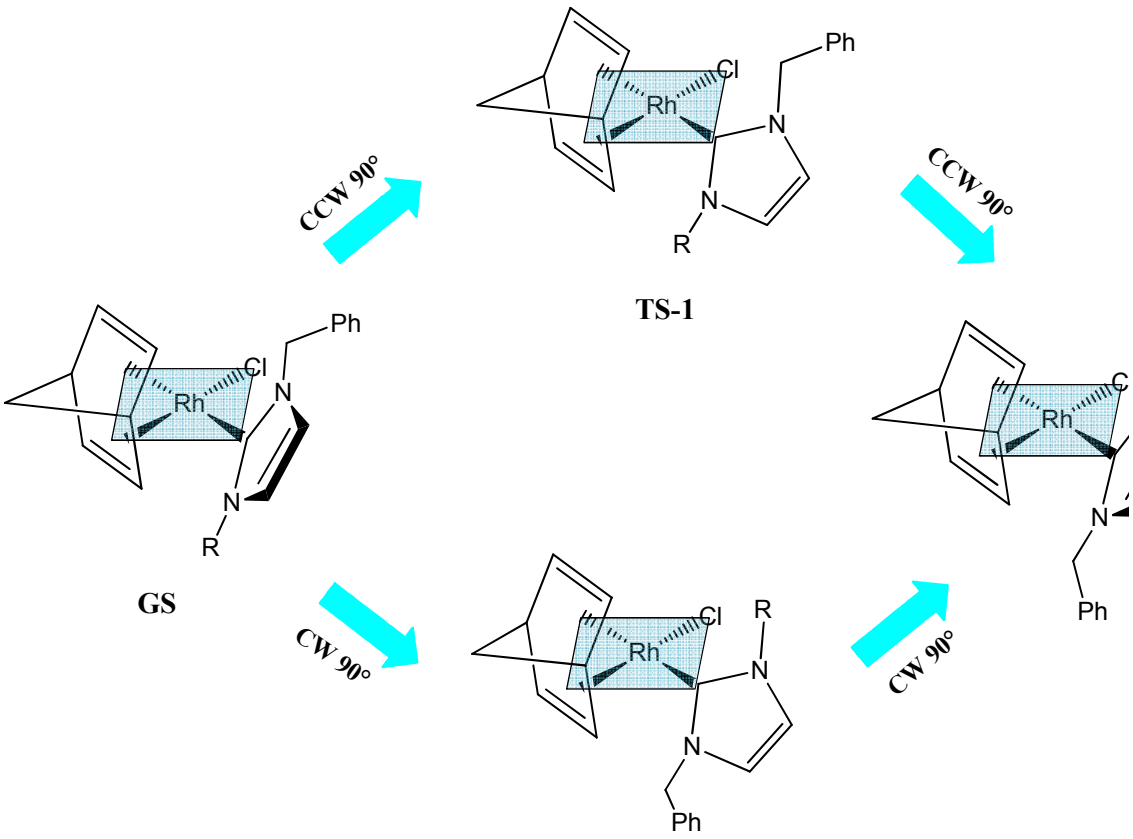

N-Heterocyclic Carbene Rhodium(I) Complexes Containing an Axis of Chirality: Dynamics and Catalysis

Maria Cristina Cassani, Marta Anna Brucka, Cristina Femoni, Michele Mancinelli, Andrea Mazzanti, Rita Mazzoni,* Gavino Solinas*

Dipartimento di Chimica Industriale "Toso-Montanari", viale Risorgimento 4, I-40136 Bologna, Italy.

Keywords: *N*-heterocyclic carbene ligands / rhodium(I) complexes / axis of chirality / NMR spectroscopy / catalysis

---

Abstract. The novel rhodium(I) complexes [RhCl(NBD)(NHC)] [NBD = norbornadiene, NHC = 1-benzyl-3-R-imidazolin-2-ylidene; R = Me (**3a**), Bz (**3b**), Tr (**3c**), ^{t}Bu (**3d**)], containing on one nitrogen the benzyl substituent and on the other increasing bulky alkyl substituents were prepared. All the complexes display restricted rotation around the metal-carbene bond and yield conformational enantiomers. The stereodynamics and racemization barriers about the Rh-carbene have been determined by means of NMR spectroscopy for **3a-c**, whereas for the bulkiest **3d** only the lower limit (91 kJ mol^{-1}) could be calculated. Whilst the racemization barriers obtained by DFT calculations for **3a**,**b** and **3d** matched the experimental values, in the case of **3c** the latter (62.3 kJ mol^{-1}) was much smaller with respect to the calculated one (101.7 kJ mol^{-1}). The lower experimental barrier has been attributed to a dissociative pathway that produces a solvated ionic pair in the transition state. The catalytic activity of the neutral rhodium(I) complexes **3a** and **3d** in the hydrosilylation with $HSiMe_2Ph$ of the terminal alkynes PhC≡CH, TolC≡CH, nBuC≡CH,

*To whom correspondence should be addressed. E-mail: maria.cassani@unibo.it (M.C.C.), rita.mazzoni@unibo.it (R.M.); fax: +39 0512093694; phone: +39 051 2093700.

$Et_3SiC{\equiv}CH$, $(CPh_2OH)C{\equiv}CH$ has been investigated, and compared with the amide-functionalized [RhCl(NBD){1-(2-NHBoc-ethyl)-3-Me-imidazolin-2-ylidene}] (**4**) and with [RhCl(NBD){1-butyl-3-Me-imidazolin-2-ylidene}] (**5**).

1. Introduction

N-Heterocyclic carbenes (NHCs) are efficient ancillary ligands because of their strong coordination ability and their tuneable character which allows the control of the steric and electronic properties on the metal centre.[1]

We recently reported the structures, dynamics and catalytic activity of rhodium(I)-NHC complexes of the type [RhX(NBD)(NHC)] [NHC = 1-(2-NHBoc-ethyl)-3-R-imidazolin-2-ylidene; R = methyl (Me), benzyl (Bz), trityl (Tr); X = Cl, I], in which the *N*-heterocyclic ligand was bearing a Boc-protected 1-(2-aminoethyl) group on one side and increasingly bulky *N*-alkyl substituents on the other (Fig. 1).[2]

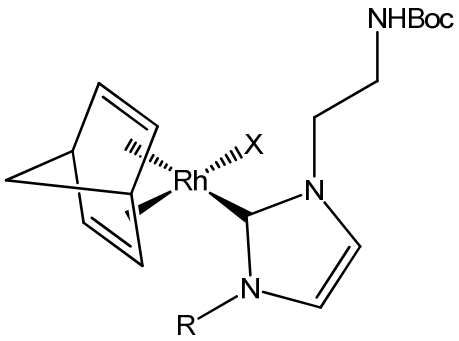

NHC - Rh	Calc. (KJ mol^{-1})	Exp. (KJ mol^{-1})
R = Me, X = Cl	58.8	55.3
R = Bz, X = Cl	67.9	58.6
R = Tr, X = Cl	100.0	58.8
R = Me, X = I	79.2	72.4

Fig. 1 *N*-Heterocylic carbene-amide rhodium(I) complexes and metal-carbene bond rotational barriers.

The catalytic activity of the neutral amide-functionalized rhodium(I) complexes in the hydrosilylation of terminal alkynes with $HSiMe_2Ph$ was also investigated. We found that the steric hindrance on the *N*-heterocyclic ligand and on the alkyne substrates affects conversion and selectivity. More specifically, for the former the best results were achieved by employing the less encumbered catalyst with TolC≡CH, whereas by using hindered alkynes such as $Et_3SiC{\equiv}CH$ or $(CPh_2OH)C{\equiv}CH$ the hydrosilylation selectively leads to the formation of the β-(E)-vinylsilane and α-bis(silyl)alkene isomers.[1d,3]

In view of these previous results, we report here a series of novel [RhCl(NBD)(NHC)] rhodium(I) complexes (NHC = 1-benzyl-3-R-imidazolin-2-ylidene; R = Me, Bz, Tr, ^{t}Bu), where a *N*-benzyl substituent was chosen as a chiral probe and the other *N*-substituent is an sp^3 carbon with

increasing bulkiness. In the hydrosilylation of terminal alkynes, a comparative study between the catalytic activity of these new systems and the previously reported Rh(I) complexes, bearing amide-functionalized NHC ligands, has been made. The purpose of this investigation was to elucidate the role played by the heteroatom functionality and the steric hindrance close to the reactive site.

2. Results and Discussion

2.1 Synthetic studies

The four imidazolium salts [BzImR]X (Im = imidazole) shown in Scheme 1 were prepared either by alkylation of 1-benzylimidazole (**1a**, **1b**)[4,5] with the pertinent alkyl halide, or by alkylation of *tert*-butylimidazole with benzyl bromide (**1d**).[6] The former synthetic procedure was also employed for the preparation of the novel imidazolium salt **1c**. The imidazolium salt **1a** is a pale yellow viscous liquid, whereas the salts **1b-d** are very hygroscopic crystalline solids. They all are soluble in chlorinated solvents such as CH_2Cl_2, $CHCl_3$, and were fully characterized by elemental analysis, NMR spectroscopy and electrospray ionization mass spectrometry (ESI-MS). The NMR resonances of **1c** were observed at chemical shifts typical for compounds of this kind, with the benzylic protons resonating at 5.97 ppm.[2]

Subsequent reaction of **1a-d** with Ag_2O in dichloromethane, carried out at room temperature with the exclusion of light, afforded the less bulky silver(I)-NHC complexes **2a**[7] and **2b**[8] after 2 h, and the more encumbered **2c** and **2d**[9] after 48 h. The complex **2c** bearing a trityl group on the NHC ligand is new and its formation was unambiguously confirmed by elemental analysis, NMR spectroscopy and ESI-MS mass spectrometry. As regards the ^{13}C NMR, it is worth mentioning that in the case of the hitherto not reported complex **2c**, the Ag-C resonance appears as a broad doublet at 185.0 ppm with a ^{13}C-$^{107/109}Ag$ coupling constant of 236 Hz, in keeping with literature data.[10]

The rhodium complexes [RhCl(NBD)(NHC)] (NBD = 2,5-norbornadiene; NHC = 1-benzyl-3-R-imidazolin-2-ylidene; **3a**: R = Me; **3b**: R = Bz; **3c**: R = Tr; **3d**: R = ^{t}Bu) were synthesized in high yields (70–90%) by transmetalation from the Ag(I)-NHC complexes **2a-d** in dichloromethane

(Scheme 1).

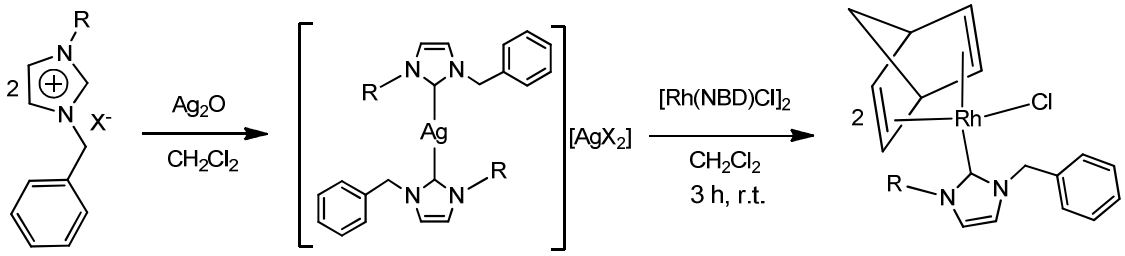

1a (R = Me), **1b** (R = Bz), **2a-d** **3a-d**

1c (R = Tr), **1d** (R = ^{t}Bu)

Scheme 1 Synthesis of Rhodium(I)-NHC complexes.

Complexes **3a-d** were isolated as yellow microcrystalline solids by gradient column chromatography under argon on anhydrous silica gel. They are completely soluble in chlorinated solvents and acetonitrile, partially soluble in diethyl ether, and completely insoluble in petroleum ether. Contrary to what observed for the previously reported amide-functionalized rhodium(I)-NHC complexes,[2] **3a-d** are air- and moisture-stable in the solid state and in solution, as confirmed by continuous monitoring of NMR samples in $CDCl_3$ over 2 weeks. Complexes **3a-d** have been fully characterized by ESI-MS mass spectrometry, ^{1}H and ^{13}C NMR using gCOSY, gHSQC, and gHMBC experiments for full resonance assignments. The most significant chemical shifts and coupling constants in ^{1}H and ^{13}C NMR spectra of **3a-d** are also summarized in Table 1S and 2S in the Supplementary Information.

The general trend which can be observed for all of the compounds **3a-d** is the increasing complexity of their ^{1}H NMR spectra (acquired at room temperature) with the increasing bulkiness of the *N*-alkyl substituents. The bigger the steric hindrance, the higher the activation energy of the rotation about the Rh-carbene bond. As an example, the signals attributed to the imidazole backbone protons (resonating at a slightly lower field with respect to the corresponding imidazolium salts and silver complexes) appear as two singlets at 6.76 and 6.65 ppm for **3a** and as one singlet at 6.61 ppm for the symmetric **3b**. However, for the more hindered **3c**,**d** the discussed protons appear as two doublets with the $^3J_{H,H} \approx 2$ Hz. At room temperature the benzylic CH_2

protons are found as singlets for the complexes **3a**,**b** (*vide infra*), whereas the CH_2 of **3c**,**d** decoalesces into an AB system, showing two doublets with the $^{2}J_{H,H} \approx 15$ Hz (Fig. 1S). The formation of the AB system is the consequence of the C_1 symmetry of the complexes in their ground state. In the NMR time scale, when the rotation about the Rh-C bond is fast (as in **3a** and **3b**) the benzylic CH_2 is a singlet, while it splits into the AB spin system when the rotation is slow. With regard to the ^{13}C NMR spectra all **3a-d** complexes show a doublet at *ca.* 180 ppm, resulting from the coupling of the carbenic carbon to the rhodium nucleus with $^{1}J(^{13}C\text{-}^{103}Rh)$ coupling constants of ca. 58 Hz (see also the Experimental part and Table 2S).

It is worth mentioning that complexes [RhCl(COD)(NHC)] having the 1,5-cyclooctadiene (COD) as ancillary ligands instead of NBD, analogous to **3a** and **3b,** have been already described. However, when R = Me[11] no dynamic behaviour was reported, whilst when R = Bz [12] two separate doublets associated with diastereotopic hydrogens of the benzyl group were observed in the ^{1}H NMR spectra, though the rotational barrier could not be measured.

2.2 Crystal Structure Determination for 3a and 3b

The molecular structures of the rhodium(I) complexes **3a** and **3b** were determined via X-ray diffraction and are illustrated in Figs. 2 and 3, while crystal data and experimental details for all structures are collected in Table 3S. Crystals of **3a**-**b** suitable for diffraction were grown from a double layer of dichloromethane and petroleum ether (1:4). The structure of **3a**, which crystallized in a centrosymmetric space group ($P2_1/c$) of the monoclinic crystal system (Z = 4), consists of separated $C_{20}H_{27}ClN_2Rh$ molecules arranged in eclipsed, alternating columns of conformational enantiomers in a 1:1 ratio. The two possible orientations of the benzyl and methyl substituents on the imidazolium ring result from the axial chirality present in the molecule of **3a**. Rhodium shows a classic square-planar coordination and is bonded to the Cl(2) atom, the carbenic C(1) and the bidentate norbornadiene fragment. There is a stronger trans effect observed for the carbene moiety when compared to the chlorine ligand. This is inferable from the difference in bond lengths between the Rh atom and the carbon atoms of the norbornadiene moiety situated in trans orientation with

respect to the chlorine and the carbene, respectively. As a matter of fact, the Rh-C(16) and Rh-C(20) contacts trans to the chlorine are 2.083(4) and 2.098(4) Å, in that order, while the Rh-C(14) and Rh-C(15) bond lengths trans to Cl atom are remarkably longer: 2.194(4) and 2.213(4) Å, correspondingly. It is worth noting that despite the presence of donor chloride anions, there are not significant intra- or intermolecular hydrogen bonds in the solid state.

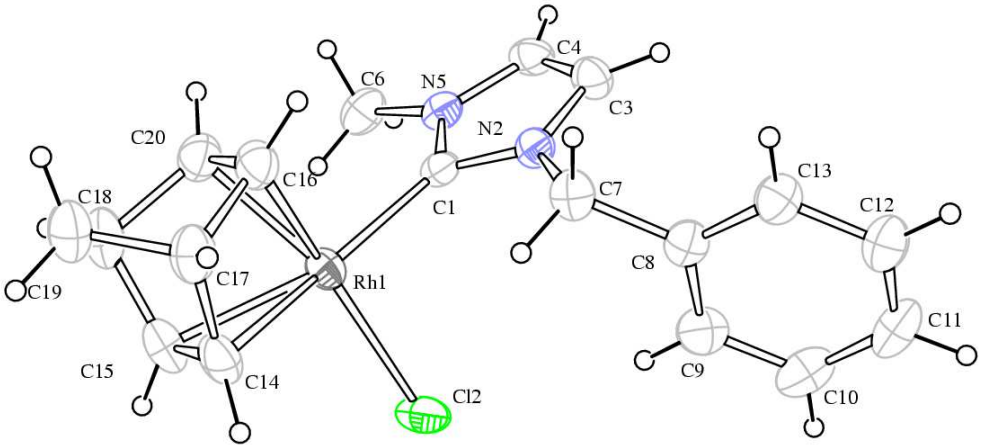

Fig. 2 ORTEP diagram of **3a** depicted with thermal ellipsoids at 30% probability.

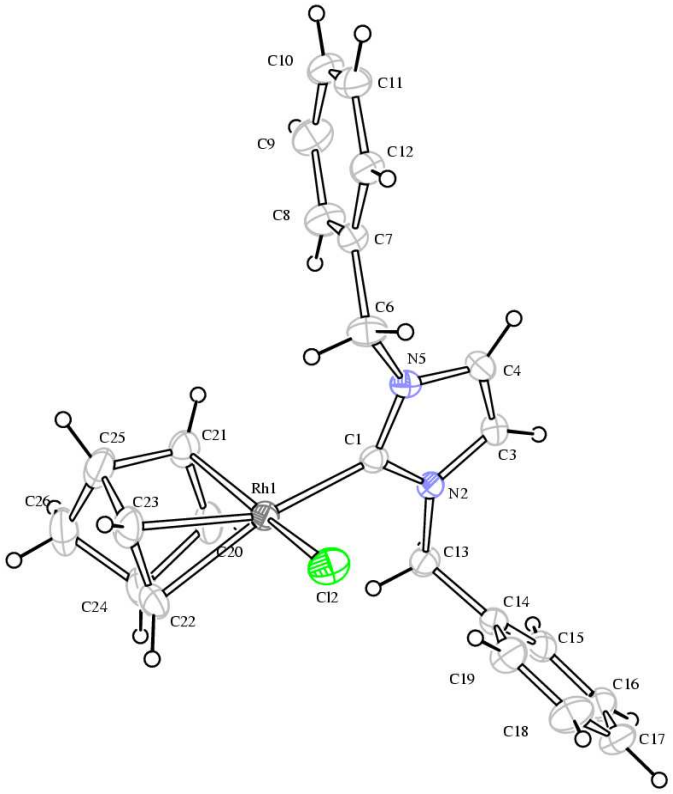

Fig. 3 ORTEP diagram of **3b** depicted with thermal ellipsoids at 30% probability.

The complex **3b** crystallizes in the centrosymmetric $P2_1/n$ group of the monoclinic crystal system (Z = 4) and both conformational enantiomers are generated by the centre of symmetry of the unit cell, as in the previous case. Similarly, there is also the trans effect observable in the structure of **3b**, with the Rh-$C_{norbornadiene}$ distances shorter when in trans orientation with respect to the carbene moiety than those being in trans to the chloride ligand. More precisely, the Rh-C(20) and Rh-C(21) contacts are 2.084(2) and 2.091(2), respectively, whereas Rh-C(22) and Rh-C(23) distances are longer: 2.185(2) and 2.195(2).

The bond distances and angles in complexes **3a** and **3b** data are quite similar. A list of the most relevant values is reported in Table 4S.

2.3 Stereodynamics

The stereodynamics and the rotational barriers about the Rh-carbene bond have been determined by means of variable-temperature (VT) NMR spectroscopy.[13] The direct consequence of the hindered rotation about the Rh–carbene bond is the lack of the symmetry plane in these complexes. The norbornadiene moiety and the chlorine atom are displaced out-of-plane with respect to the imidazole ring. Being the two-side arms different, the molecule belongs to the C_1 symmetry point group; therefore a pair of conformational enantiomers is generated (Fig. 4).[14]

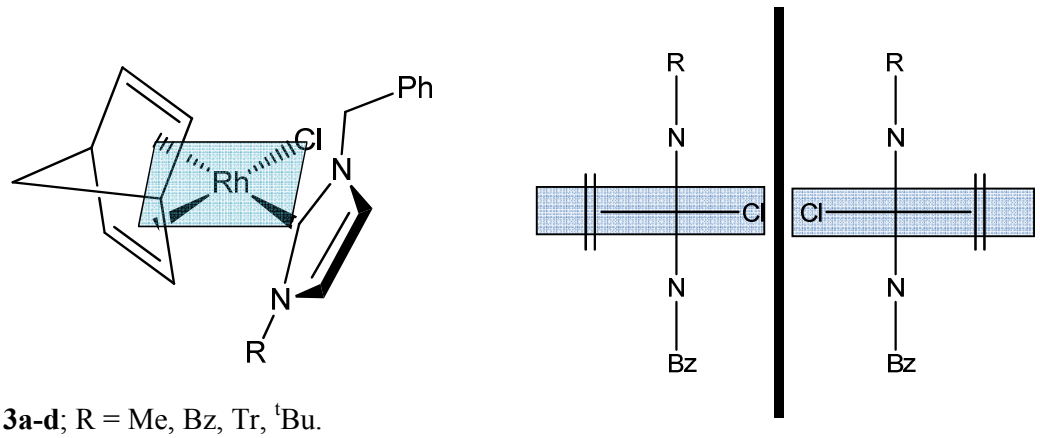

3a-d; R = Me, Bz, Tr, ^{t}Bu.

Fig. 4 Coordination plane of the rhodium(I) in the complexes **3a-d** and the two conformational enantiomers generated by the chiral axis along the Rh-carbene bond.

The interconversion pathway of the two enantiomeric conformers is shown in Scheme 2. The two enantiomeric ground states GS and GS' can interconvert into each other by two possible transition states, due to the rotation around the carbene-rhodium bond.

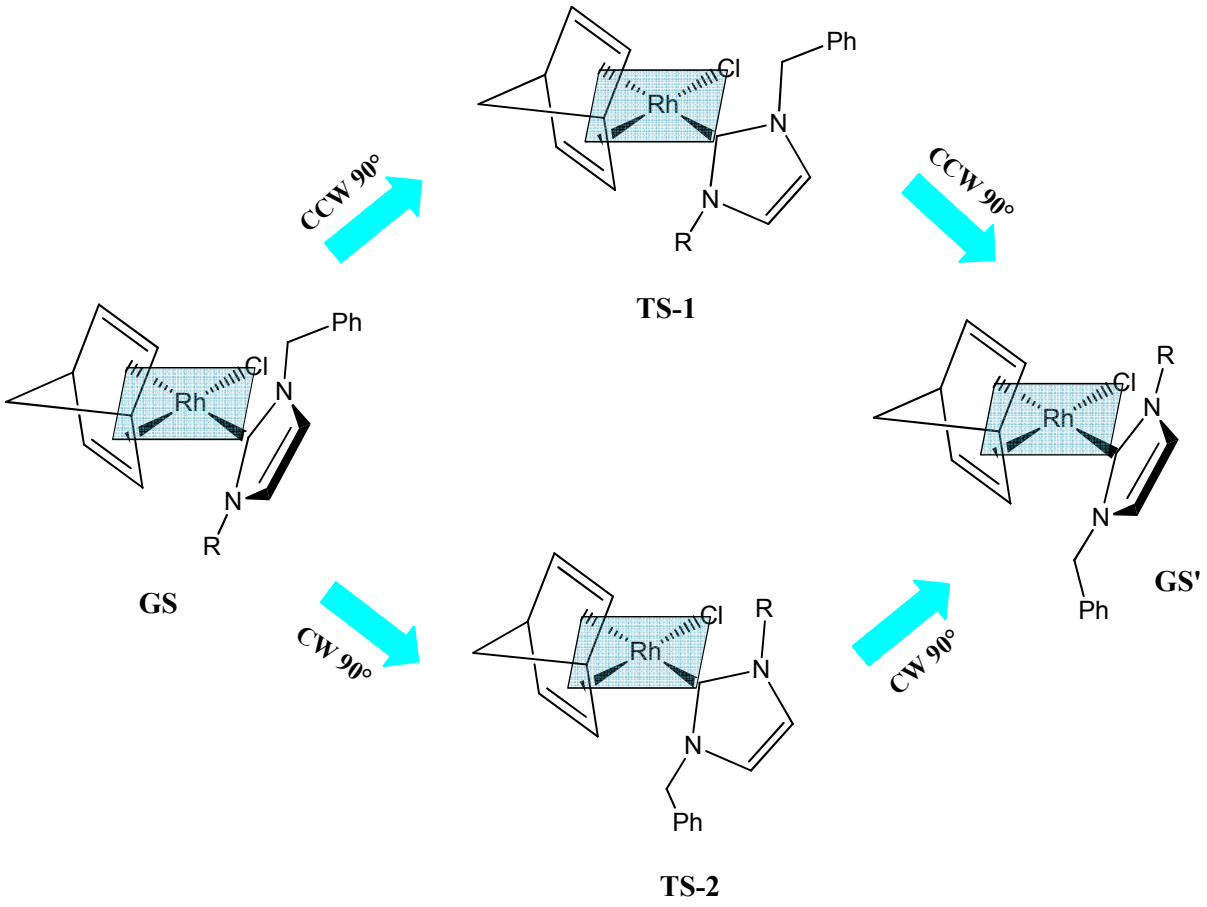

Scheme 2 Enantiomerization pathway for compounds **3a-d**; R = Me, Bz, Tr, ^{t}Bu.

The first transition state (TS-1) is reached from GS by a 90° counter clockwise rotation of the imidazole and corresponds to the crossing of the chlorine atom on the benzylic CH_2 of one of the side arms of the imidazole. The second transition state (TS-2) takes place when a clockwise rotation forces the chlorine atom to cross the second alkyl side arm group (R) on the imidazole. The steric hindrance of R obviously influences the activation energy of the rotational barrier. DFT calculations of the two possible transition states (Table 1), performed at the B3LYP/LANL2DZ level, suggested that the threshold pathway (*i.e.*, that with the lowest transition-state energy) corresponds in all cases to the passage of the halogen atom on the benzyl group (TS-1), with the simultaneous crossing of the norbornadiene on the second side arm (R).

The *N*-benzyl group on one side of the imidazole was chosen as probe of chirality, because its enantiotopic geminal protons become diastereotopic in presence of a chiral axis giving a characteristic AB system.[15] In addition, the CH_2 signals are in a free area of the ^1H spectrum, thus allowing a reliable simulation of the line shape. The ^1H NMR spectra of the complex **3a** recorded in the -35 to 25 °C range (1,1,2,2-tetrachloroethane-d_2) are shown in Fig. 5 (left). The single signal of the benzylic geminal protons at 5.73 ppm broadened on decreasing the temperature and reached the coalescence at +10 °C. On further lowering the temperature, it splits into the expected AB system, showing sharp lines at -35 °C (5.60 and 5.85 ppm, J = 15.0 Hz).

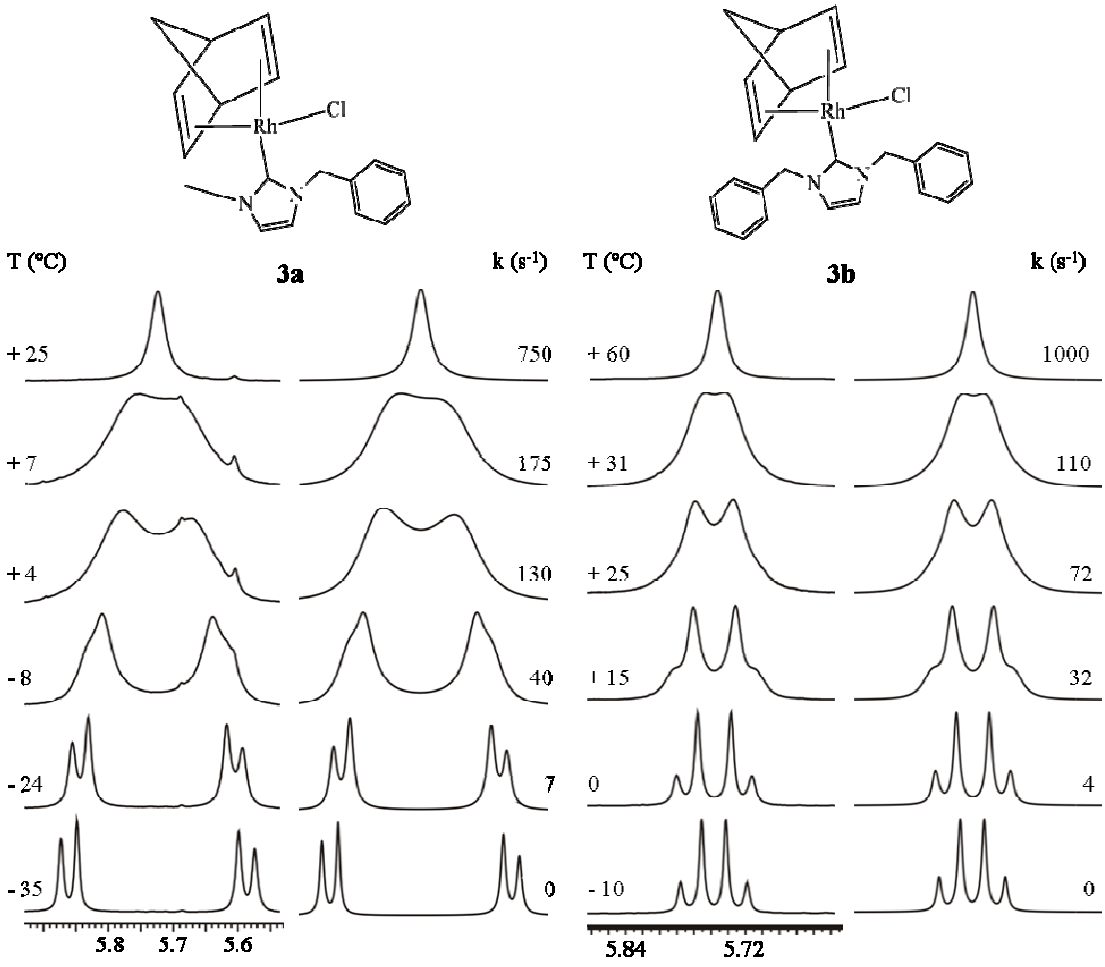

Fig. 5 Variable-temperature spectra of **3a** and **3b** showing the evolution of the benzylic CH_2 signals (^1H NMR at 600 MHz, $C_2D_2Cl_4$). On the right side of each plot the simulations with the corresponding rate constants are reported.

Line shape simulation at various temperatures yielded the rate constants for the enantiomerization process, from which an activation energy of 56.5 kJ mol^{-1} was derived by the Eyring equation (Table 1).

Table 1 Calculated and experimental energy barriers for the enantiomerization of **3a-d** (energies in kJ mol^{-1}, calculations at the B3LYP/LANL2DZ level).

Compound	TS-1	TS-2	Experimental $\Delta G^{\ddagger}$ (kJ mol^{-1})
3a	55.0	58.5	56.5
3b	65.3	78.7	62.7
3c	101.7	115.9	62.3[a]
3d	96.7	119.7	> 91

[a] $\Delta H^{\ddagger}$ value.

In complex **3b** the two benzyl groups on the N-side arms of the imidazole caused a bigger steric hindrance with respect to the previously discussed **3a**, in that the benzylic protons appeared anisochronous as a broad doublet at room temperature, and the coalescence was reached at +32 °C. On further raising the temperature, the signal sharpened and at +75 °C it exhibited a very sharp singlet. On the other hand, at -10 °C, the splitting pattern characteristic for the AB system was observed (Fig. 5, right). Although in this case the ground state has C_s symmetry, the CH_2 signals are split into an AB system because the symmetry plane of the molecule is not coincident with the local symmetry plane of the CH_2. An energy barrier of 62.7 kJ mol^{-1} was derived by line-shape simulation (Table 1). As usual in conformational processes, the energy barriers measured for **3a** and **3b** did not change with the temperature, thus implying a very small activation entropy. This suggests that the observed barrier should be driven by steric effects only, and it is consistent with the increase of the activation energy between the less sterically hindered **3a** and **3b** ($\Delta\Delta G^{\ddagger}$ = 6.2 kJ mol^{-1}). These data very well agree with those reported by Enders and Gielen,[16] who proposed a steric origin of the rotational barrier.

In the case of complex **3c** bearing the trityl group, high temperature VT experiments cannot be acquired because a decomposition processes took place before reaching the coalescence. To calculate the energy barrier, an exchange spectroscopy (EXSY) experiment has been employed. The

1D EXSY experiments[17] were carried out at four different temperatures (-10, -15, -20 and -25 °C) on the complex **3c**. The linear functions of $\ln([A]_{eq}-[A]_t)$ vs. the mixing time (25, 50, 75 and 100 ms) were plotted for each temperature (Fig. 6a), providing the kinetic constants for the Rh-C rotation. For each temperature, the activation energy was then derived by the Eyring equation.

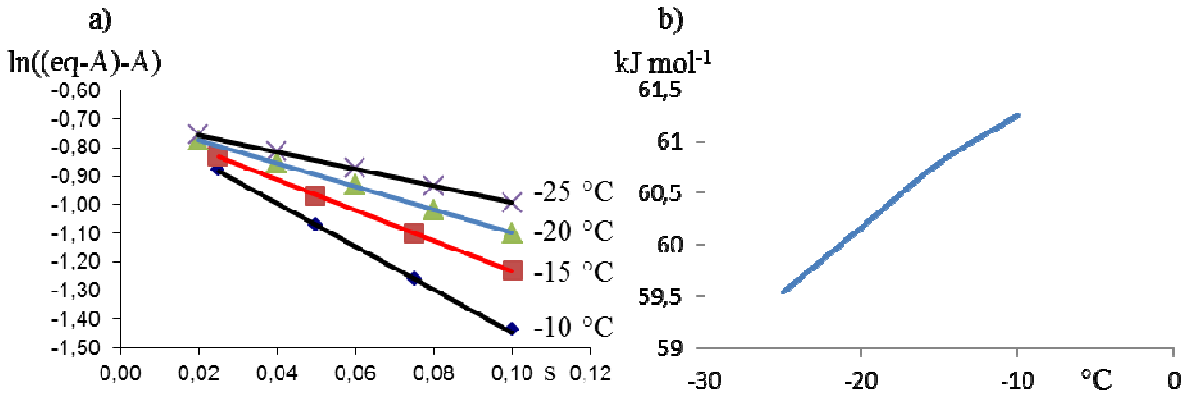

Fig. 6 (a) Plots of $\ln([A]_{eq}-[A]_t)$ vs. mixing time at different temperatures and (b) the dependence of the activation energy on the temperature.

The plot of $\Delta G^{\ddagger}$ against temperature (Fig. 6b) showed a marked increase of the activation energy, indicating a substantial and negative activation entropy. In particular, the EXSY experiment showed that the activation enthalpy $\Delta H^{\ddagger}$ (62.3 kJ mol^{-1}) was identical, within the experimental error, to the barrier derived in the case of the dibenzyl-substituted compound **3b**.

The large negative activation entropy (-115 ± 10 $JK^{-1}mol^{-1}$) suggested that a strongly organized transition state takes place in the case of compound **3c**,[18] a different interconversion pathway being the only available option. The two following hypotheses can be formulated. For the first one the lower barrier could be the result of dynamic gearing between the rotation of the rhodium-carbene and the trityl group. Such situation is well known to generate a single transition state with lower activation energy with respect to the rotation of the single groups.[19] For the second hypothesis a process involving a bond cleavage followed by subsequent regeneration of the bond can be conceived and, although it is known that such process yields a positive entropy,[20] in the present case the trityl dissociation produces two charged sub-units. The stabilization of two charged counterparts involves a much higher ordering of solvent molecules and hence lead to a negative

entropy of activation.[21] Since the correlated motion is predicted to have a large barrier, which does not match the experimental value, in our opinion the second hypothesis (two solvated ionic partners in the transition state) appears to be the correct one.

In case of complex **3d**, the high activation energy, due to the presence of the sterically demanding ^{t}Bu group, prevented the observation of the coalescence of the benzylic protons, and both VT spectra and EXSY approaches appeared to be unsuitable for the experimental determination of the kinetic data. Being the highest workable temperature about +70 °C, only a lower limit for the barrier could be calculated. If a 0.1 s^{-1} rate constant at +70 °C is considered, the corresponding energy barrier is 91 kJ mol^{-1}. This value suggests that the two conformational enantiomers could be sufficiently stable at room temperature to be observed with a different technique such as dynamic HPLC.[22] Unfortunately, any attempt to observe separate or exchanging peaks on HPLC enantioselective columns was unsuccessful because of chemical degradation of the complex in those conditions.

2.4 Hydrosilylation of terminal alkynes

Complexes **3a** and **3d**, respectively representing the less and the more hindered rhodium species, were chosen to evaluate the catalytic performance in the hydrosilylation of the following terminal alkynes: phenylacetylene, tolylacetylene, 1-hexyne, (triethylsilyl)acetylene, and 1,1-diphenyl-2-propyn-1-ol. The catalytic reactions were carried out in $CDCl_3$ using a slight excess of $HSiMe_2Ph$ and were routinely monitored by ^{1}H-NMR spectroscopy. The results have been compared with those previously reported for [Rh(NBD)Cl{1-(2-NHBoc-ethyl)-3-Me-imidazolin-2-ylidene}] (**4**)[2] and also with [Rh(NBD)Cl{1-butyl-3-Me-imidazolin-2-ylidene}] (**5**), in order to shed light on the role of the -NHBoc substituent on both the catalytic activity and selectivity. Complex **5** was prepared following the procedure described for the parent compound bearing a COD ancillary ligand.[23] Complexes under studies are summarized in Chart 1.

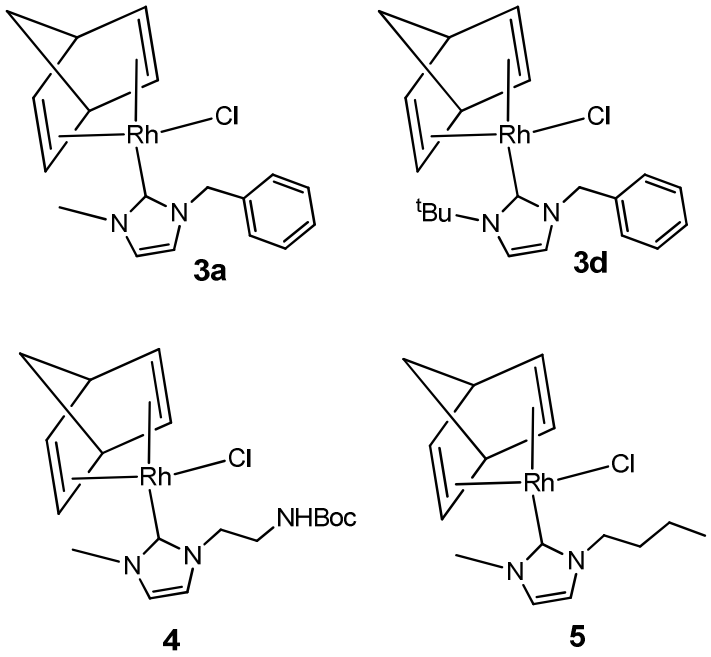

Chart 1 [RhCl(NBD)(NHC)] complexes employed in the hydrosilylation of phenylacetylene and tolylacetylene.

Conversions versus time for the hydrosilylation reaction of phenylacetylene performed at 25 °C with a catalyst loading of 1% are presented in Fig. 7, which shows that all rhodium complexes completely convert the substrate.

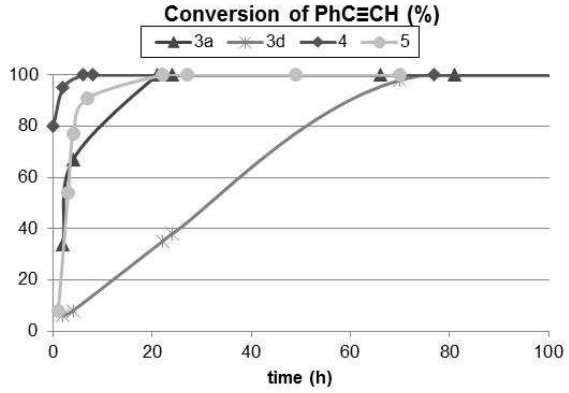

Fig. 7 Reaction profile of conversion vs time for the hydrosilylation of PhC≡CH at 25°C with **3a**, **3d**, **4** and **5**: catalyst loading of 1%.

Although the general behaviour of the conversion profiles confirms that the reaction rate is affected by steric encumbrance,[2] comparison of the turn over frequency (TOF) between **4** (48 h^{-1}) and **5** (27

h^{-1})[24] clearly demonstrated the beneficial effect of the amide-Boc group, which provides a dynamic chelating effect on the metal centre during the catalytic cycle.[1j,3a,25] When the methyl group on the NHC ligand of **4** is replaced with a benzyl group (see Fig. 1, R = Bz),[2] the TOF decreases down to 40 h^{-1} and remains significantly higher than the one registered for the less encumbered **5**. A similar behaviour was observed for the hydrosilylation of the other substrates (Fig. 3S-6S). As previously reported,[2] for 1-hexyne and 1,1-diphenyl-2-propyn-1-ol we again observed longer initiation times. Such behaviours have been ascribed to an electronic effect for the former and to the steric hindrance for the latter substrate.[3a,26,27]

With regard to the selectivity, as generally reported for transition metal catalyzed hydrosilylation of 1-alkynes,[28] and for Rh(I)NHC hydrosilylation catalysts in particular,[3a] the reaction is non-selective. As a matter of fact, the NMR analyses on the reaction products obtained by employing complexes **3a**, **3d** and **5** are in agreement with literature data[3a] and with what previously reported for **4**.[2] As shown in Scheme 3 the catalysts convert phenylacetylene and tolylacetylene into a mixture of the three possible isomeric vinylsilane derivatives: β(*Z*) or β(*E*) 1-silyl-1-alkenes (anti-Markovnikov addition), and α–2-silyl-1-alkene (Markovnikov addition). Furthermore the formation of the corresponding alkene is observed.

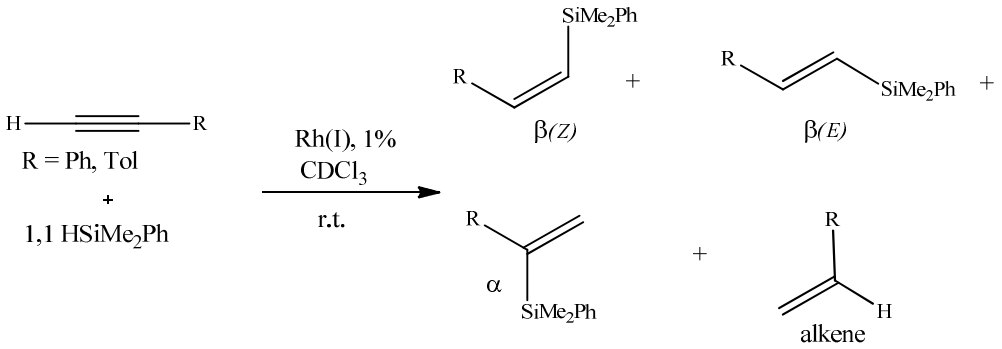

Scheme 3 Hydrosilylation of PhC≡CH and TolC≡CH with Rh(I) complexes.

The β-(*Z*) vinylsilane is the major product until the substrate completely disappears. Once reached the complete conversion β-(*Z*) isomerizes to β-(*E*) vinylsilane which, at the end of the reaction, is

always the major product. The formation of the termodinamically less stable β-(*Z*) isomer has been described in detail by Oro *et al*.[3a] using a modified Chalk-Harrod mechanism, whereas the ensuing (*Z*)-(*E*) isomerization (favoured by the presence of a slight excess of hydrosilane) has been already widely described in the literature.[29] In Fig. 8 an example of conversion and selectivity profiles vs. time for the reaction of PhC≡CH and dimethylphenylsilane mediated by the catalyst **3a** is reported.

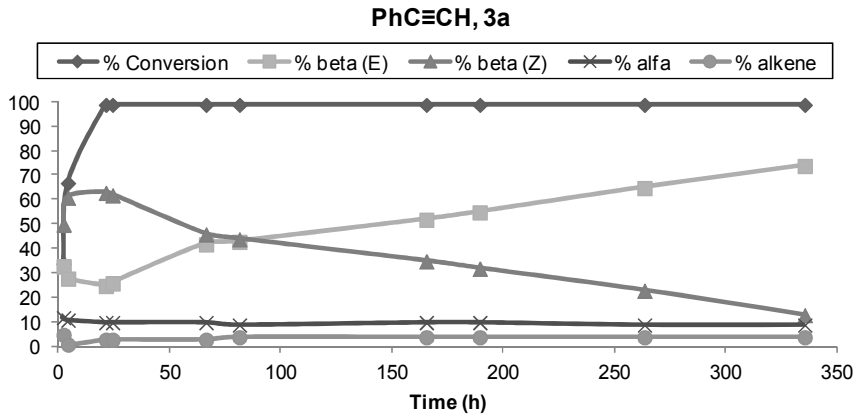

Fig. 8 Reaction profile of conversion and selectivity vs. time for the hydrosilylation of PhC≡CH with **3a**; catalyst loading 1%.

The bar diagrams in Fig. 9 for phenylacetylene and Fig. 7S for tolylacetylene summarize the data for all the catalysts under study and show that α isomer is always identified in variable amounts, 5-16%, while the alkene formation occurs in the range 0-12%.

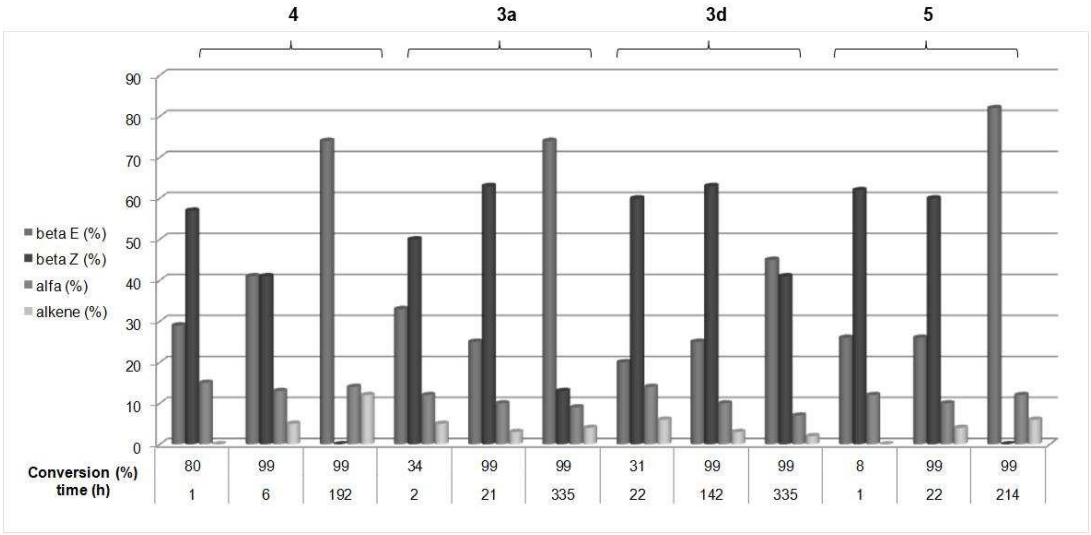

Fig. 9 Selectivity vs. conversion and time for the hydrosilylation of phenylacetylene catalyzed by **3a**, **3d**, **4** and **5**. Catalyst loading of 1%.

The experimental data obtained for the other substrates (reported in the Supporting Information) shows that the α isomer is always present, while the alkene formation occurs only with phenyl and tolylacetylene substrates.

When ^{n}BuC≡CH is employed once the conversion is complete, the *β*-(Z) vinylsilane isomerizes into the hex-2-enyl-dimethyl-phenyl-silane ((Scheme 1S, Fig.s 8S,9S) instead of the *β*-(E) vinylsilane. This behaviour is in line with what previously reported by Crabtree et al. in the hydrosilylation of 1-hexyne with $HSiMePh_2$ catalyzed by $[RhCl(PPh_3)_3]$.[30]

Finally the catalyzed reaction of dimethylphenylsilane with (triethylsilyl)acetylene and 1,1-diphenyl-2-propyn-1-ol leads to the formation of only the two isomers *β-(E)* and *α* (Scheme 2S, Fig.s 10S,11S), confirming the importance of both the steric hindrance and the electronic characteristics of the precursor.

In order to further investigate how the catalytic performance may be affected by the catalyst loading or by the temperature, the catalytic activity of **3a** in the hydrosilylation of phenylacetylene and tolylacetylene has been examined under the following conditions: 0.1%, 25 °C; 0.1%, 60 °C. At room temperature the reaction still occurred with both substrates (Fig. 12S for phenylacetylene; Fig. 13S for tolylacetylene), but slower kinetics were found (phenylacetylene was identified in the reaction mixture even after 800 h); at the same time selectivity did not show any significant improvement. Even though the reaction with tolylacetylene confirmed to be faster (the conversion was complete within 660 h, Fig. 13S), in both cases a long induction time is required: after 8 hours no conversion was observed. Finally, raising the temperature to 60 °C improves the reaction rates (Figs. 14S and 15S) but negatively affects, to some extent, the reaction selectivity.

3. Conclusions

We have described the synthesis of the novel rhodium(I) complexes [RhCl(NBD)(NHC)] [NHC = 1-benzyl-3-R-imidazolin-2-ylidene; R = Me (**3a**), Bz (**3b**), Tr (**3c**), ^{t}Bu (**3d**)], in which the NHC ligands bear a benzyl substituent on one nitrogen and increasing bulky alkyl substituents on the other. All complexes display restricted rotation about the metal-carbene bond. By using the *N*-benzyl group as chiral probe, the racemization barriers about the Rh-carbene have been determined by employing the following NMR spectroscopic techniques: VT for **3a,b** (56.5 and 62.7 kJ mol^{-1}) and EXSY for **3c** (62.3 kJ mol^{-1}); for the bulkiest **3d** only a lower limit for the rotational barrier (91 kJ mol^{-}1) could be determined. Whilst the calculated rotation barriers for **3a**,**b** and **3d** matched the experimental values, in the case of **3c** the latter (62.3 kJ mol^{-1}) was much smaller with respect to the calculated one (101.7 kJ mol^{-1}). This lower experimental energy barrier, its strong dependence from the temperature, and the large negative activation entropy derived from simulations (-115 ± 10 JK^{-1}mol^{-1}), have been attributed to a partial dissociation of the *N*-trityl to form a solvated ionic pair in the transition state.

The catalytic activity of the neutral rhodium(I) complexes **3a** and **3d** in the hydrosilylation of terminal alkynes with $HSiMe_2Ph$ has been investigated and compared with the amide-functionalized [RhCl(NBD){1-(2-NHBoc-ethyl)-3-Me-imidazolin-2-ylidene}] (**4**) and with [RhCl(NBD){1-butyl-3-Me-imidazolin-2-ylidene}] (**5**). This study has demonstrated the beneficial influence on the catalytic activity of [RhCl (NBD)(NHC)] complexes of an amide functionality on the side chain, and has confirmed that steric hindrance on the *N*-heterocyclic ligand and on the alkyne substrates affects conversion and selectivity.

4. Experimental Section

4.1 Materials and Procedures

All reactions were carried out under Argon using standard Schlenk techniques. Solvents were dried and distilled under nitrogen prior to use; the deuterated solvents used after being appropriately dried and degassed were stored in ampoules under argon on 4Å molecular sieves. The prepared

derivatives were characterized by elemental analysis and spectroscopic methods. The NMR spectra were recorded using Varian Inova (^{1}H, 300.1; ^{13}C, 75.5 MHz), Varian Mercury VX (^{1}H, 399.9; ^{13}C, 100.6 MHz), Varian Inova (^{1}H, 599.7, ^{13}C, 150.8 MHz) spectrometers; chemical shifts were referenced internally to residual solvent peaks for ^{1}H ($CDCl_3$: 7.26 ppm) and ^{13}C NMR ($CDCl_3$: 77.00 ppm) spectra. Spectra have been edited with the software MestReNova Version: 8.0.2-11021, 2012 Mestrelab Research S.L. and unless otherwise stated, they were recorded at 298 K for characterization purposes; full ^{1}H and ^{13}C NMR assignments were done, when necessary, by gCOSY, gHSQC, gHMBC, NOESY and DEPT-135 NMR experiments using standard Varian pulse sequences; J.Young valve NMR tubes (Wilmad) were used to carry out NMR experiments under inert conditions. ESI-MS analyses were performed by direct injection of methanol solutions of the metal complexes using a WATERS ZQ 4000 mass spectrometer. Elemental analyses were performed on a ThermoQuest Flash 1112 Series EA Instrument. The chemicals 1-methylimidazole, 1-benzylimidazole, benzyl bromide, tert-butyl bromide, 1-butyl-3-methyl-imidazolium bromide, phenylacetylene, tolylacetylene, 1-hexyne, triethylsililacetylene, 1,1-diphenyl-2-propyn-1-ol, $HSiMe_2Ph$ and Ag_2O were used as purchased from Aldrich; $[Rh(NBD)Cl]_2$ was purchased from Strem and used as received. The starting building blocks 1-tert-butylimidazole,[31] trityl chloride,[2] 1-benzyl-3-methyl-imidazolium bromide (**1a**),[4] 1,3-dibenzyl-imidazolium bromide (**1b**),[5] 1-benzyl-3-tert-butylimidazolium bromide (**1d**),[6] 1-benzyl-3-methyl-imidazolin-2-ylidene silver bromide (**2a**),[7] 1,3-dibenzyl-imidazolin-2-ylidene silver bromide (**2b**),[8] 1-benzyl-3-*tert*-butyl-imidazolin-2-ylidene silver bromide (**2d**),[9] [RhCl(NBD){1-(2-NHBoc-ethyl)-3-Me-imidazolin-2-ylidene}] (**4**)[2] were prepared according to literature procedures and the syntheses are also reported in the Supplementary Information. Petroleum ether (Etp) refers to a fraction of bp 60-80 °C. The reactions were monitored by thin-layer chromatography (TLC) on highly purified silica gel on polyester (w/UV indicator) and visualized using UV light (254 nm). Column chromatography was carried out under argon on silica gel previously heated at about 200 ºC while a slow stream of a dry nitrogen was passed through it;[32] celite was dried in an oven at 150 °C.

4.2 Syntheses

4.2.1 1-benzyl-3-trityl-imidazolium chloride (1c). In a Schlenk tube to a solution of trityl chloride (0.18 g, 0.64 mmol) dissolved in CH_2Cl_2 (10 mL), 1-benzylimidazole (0.10 g, 0.65 mmol) was added. After stirring for 16 h at room temperature, the solvent was removed under vacuum and the resulting solid was thoroughly washed with diethyl ether (3 x 10 mL) to yield **1c** as a white solid (0.25 g, 89%). ^{1}H NMR (300.1 MHz, $CDCl_3$): δ 9.92 (s, 1H, NCHN), 7.65 (s, 1H, CH_{im}), 7.49–7.11 (m, 20H, Ph), 6.93 (s, 1H, CH_{im}), 5.97 (s, 2H, CH_2Ph). ^{13}C NMR (75.5 MHz, $CDCl_3$): δ 139.6 (C_5), 138.3 (NCHN), 133.5 (C_q, benzyl), 129.6-127.7 (Ph), 123.7 (CH_{im}), 121.8 (CH_{im}), 79.8 (C_1), 53.9 (CH_2Ph). ESI-MS (MeOH, *m/z*): 401 (100) $[M - Cl]^+$; In the ESI-MS(-) spectrum, no peaks were observed. Anal. Calcd (%) for $C_{29}H_{25}ClN_2$: C, 79.71; H, 5.77; N, 6.41. Found: C, 79.67; H, 5.71; N, 6.39.

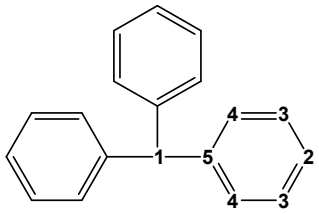

Trityl group numbering scheme

4.2.2 1-benzyl-3-trityl-imidazolin-2-ylidene silver bromide (2c). To a solution of **1c** (0.23 g, 0.53 mmol) in CH_2Cl_2 (ca. 10 mL) stirred in a Schlenk, Ag_2O (0.07 g, 0.30 mmol) was added. The suspension was stirred for 48 h at room temperature and then filtered on Celite; the colourless filtrate was characterised by NMR and then straightforwardly used for the preparation of the corresponding rhodium complex **3c**. ^{1}H NMR (300.1 MHz, $CDCl_3$): δ 7.34–7.21 (m, 20H, Ph), 7.03 (d, 1H, $^3J_{H,H}$ = 1.9 Hz, CH_{im}), 6.91 (d, 1H, $^3J_{H,H}$ = 1.9 Hz, CH_{im}), 5.25 (s, 2H, CH_2Ph). ^{13}C NMR (75.5 MHz, $CDCl_3$): δ 185.1 (d, $J_{Ag,C}$ = 236.0 Hz, C-Ag), 141.9 (C_5), 135.4 (C_q, benzyl), 129.8 (Ph), 128.9 (Ph), 128.4 (Ph), 128.2 (Ph), 127.8 (Ph), 127.7 (Ph), 127.6 (Ph), 127.0 (Ph), 123.8 (CH_{im}), 118.9 (CH_{im}), 77.7 (C_1), 56.8 (CH_2Ph).

4.2.3 [RhCl(NBD){1-benzyl-3-methyl-imidazolin-2- ylidene}] (3a). The *in situ* prepared silver complex **2a** was added to a solution of $[Rh(NBD)Cl]_2$ (0.12 g, 0.26 mmol) in CH_2Cl_2. After stirring for 3 h at room temperature, the pale yellow AgBr was filtered off, and the solvent was removed under vacuum. The crude material was purified by column chromatography on silica gel using first CH_2Cl_2 and then CH_2Cl_2/MeOH [100:3 (v/v)] as eluent to afford **3a** as a yellow solid (0.15 g, 72 %). R_f: 0.33 (CH_2Cl_2/MeOH, 100:3). ^{1}H NMR (300.1 MHz, $CDCl_3$): δ 7.35 (m, 5H, Ph), 6.76 (s, 1H, CH_{im}), 6.65 (s, 1H, CH_{im}), 5.72 (s, 2H, CH_2Ph), 4.84 (s, 2H, NBD), 4.08 (s, 3H, CH_3), 3.72 (s, 2H, NBD), 3.36 (br s, 2H, NBD), 1.30 (m, 2H, NBD). ^{13}C NMR (75.5 MHz, $CDCl_3$): δ 184.8 (d, $J_{C,Rh}$ = 57.8 Hz), 136.9 (C_q, Ph), 128.8 (Ph), 128.3 (Ph), 128.1 (Ph), 122.2 (CH_{im}), 120.7 (CH_{im}), 79.0 (d, $J_{C,Rh}$ = 6.0 Hz, NBD), 63.4 (d, $J_{C,Rh}$ = 5.2 Hz, NBD), 54.3 (CH_2Ph), 51.0 (d, $J_{C,Rh}$ = 2.5 Hz, NBD), 48.3 (d, $J_{C,Rh}$ = 12.8 Hz, NBD), 37.8 (CH_3). ESI-MS (MeOH, *m/z*): 367 (30) $[M - Cl]^+$; 539 (100) $[Rh(NBD)(NHC)_2]^+$. Anal. Calcd (%) for $C_{18}H_{20}ClN_2Rh$: C, 53.68; H, 5.01; N, 6.96. Found: C, 53.59; H, 5.08; N, 6.94.

4.2.4 [RhCl(NBD){1,3-dibenzyl-imidazolin-2-ylidene}] (3b). The *in situ* prepared silver complex **2b** was added to a solution of $[Rh(NBD)Cl]_2$ (0.14 g, 0.30 mmol) in CH_2Cl_2. After stirring for 3 h the pale yellow AgBr was filtered off, and the solvent was removed under vacuum. The crude material was purified by column chromatography on silica gel using first CH_2Cl_2 and then

CH_2Cl_2/MeOH [100:3 (v/v)] as eluent to afford **3b** as a yellow solid (0.25 g, 86%). R_f: 0.45 (CH_2Cl_2/MeOH, 100:3). ^{1}H NMR (300.1 MHz, $CDCl_3$): δ 7.31 (m, 10H, Ph), 6.61 (s, 2H, CH_{im}), 5.73 (br s, 4H, CH_2Ph), 4.78 (br s, 2H, NBD), 3.60 (br s, 2H, NBD), 3.20 (br s, 2H, NBD), 1.20 (br s, 2H, NBD). ^{13}C NMR (75.5 MHz, $CDCl_3$): δ 185.4 (d, $J_{C,Rh}$ = 58.3 Hz), 136.9 (C_q, Ph), 128.9 (Ph), 128.6 (Ph), 128.03 (Ph), 121.1 (CH_{im}), 120.72 (CH_{im}), 79.1 (d, $J_{C,Rh}$ = 5.7 Hz, NBD), 63.3 (d, $J_{C,Rh}$ = 5.3 Hz, NBD), 54.5 (CH_2Ph), 51.0 (d, $J_{C,Rh}$ = 2.0 Hz, NBD), 48.5 (d, $J_{C,Rh}$ = 17.0 Hz, NBD). ESI-MS (MeOH, *m/z*): 443 (100) $[M - Cl]^+$. Anal. Calcd (%) for $C_{24}H_{24}ClN_2Rh$: C, 60.20; H, 5.05; N, 5.85. Found: C, 60.15; H, 5.09; N, 5.93.

4.2.5 [RhCl(NBD) {1-benzyl-3-trityl-imidazolin-2-ylidene}] (3c). The *in situ* prepared silver complex **2c**, was added to a solution of $[Rh(NBD)Cl]_2$ (0.15 g, 0.32 mmol) in CH_2Cl_2. After stirring for 3 h the white AgCl was filtered off, and the solvent was removed under vacuum. The crude material was purified by column chromatography on silica gel treated with 5% v/v triethylamine in diethyl ether, using Et_2O/CH_2Cl_2, 1:1 v/v, to afford **3c** as a yellow solid (0.28 g, 70 %). R_f: 0.55 (Et_2O/CH_2Cl_2, 50:50). ^{1}H NMR (300.1 MHz, $CDCl_3$): δ 7.45–7.24 (m, 20H, Ph), 6.84 (d, 1H, $^2J_{H,H}$ = 14.9 Hz, CH_2Ph), 6.76 (d, 1H, $^3J_{H,H}$ = 2.0 Hz, CH_{Im}), 6.56 (d, 1H, $^3J_{H,H}$ = 2.0 Hz, CH_{Im}), 6.17 (d, 1H, $^2J_{H,H}$ = 14.9 Hz, CH_2Ph), 4.61 (br s, 1H, NBD), 3.59 (br s, 1H, NBD), 3.44 (br s, 1H, NBD), 3.10 (br s, 1H, NBD), 2.87 (br s, 1H, NBD), 1.94 (br s, 1H, NBD), 0.87 (m, 2H, NBD). ^{13}C NMR (75.5 MHz, $CDCl_3$): δ 186.6 (d, $J_{C,Rh}$ = 55.1 Hz), 142.4 (C_5), 137.5 (C_q, benzyl), 129.1 (Ph), 128.9 (Ph), 128.3 (Ph), 128.1 (Ph), 127.9 (Ph), 127.5 (Ph), 127.2 (Ph), 124.3 (CH_{im}), 120.7 (CH_{im}), 76.6 (C_1), 73.1 (s, NBD), 61.8 (d, $J_{C,Rh}$ = 5.8 Hz, NBD), 57.2 (CH_2Ph), 49.7 (NBD), 49.0 (NBD), 45.7 (d, $J_{C,Rh}$ = 13.0 Hz, NBD), 44.74 (d, $J_{C,Rh}$ = 10.8 Hz, NBD). ESI-MS (MeOH, *m/z*): 595 (100) $[M - Cl]^+$. Anal. Calcd (%) for $C_{36}H_{32}ClN_2Rh$: C, 68.52; H, 5.11; N, 4.44. Found: C, 68.39; H, 5.21; N, 4.44.

4.2.6 [Rh(NBD)Cl{1-benzyl-3-tert-butyl-imidazolin-2- ylidene}] (3d). The *in situ* prepared silver complex **2d** was added to a solution of $[Rh(NBD)Cl]_2$ (0.25 g, 0.54 mmol) in CH_2Cl_2. After stirring for 4 h the pale yellow AgBr was filtered off, and the solvent was removed under vacuum. The

crude material was purified by column chromatography on silica gel treated with 5% v/v triethylamine in diethyl ether, using first CH_2Cl_2 and then CH_2Cl_2/MeOH [100:2 (v/v)] as eluent to afford **3c** as a yellow solid (0.36 g, 75 %). R_f: 0.51 (CH_2Cl_2/MeOH, 100:7). ^{1}H NMR (599.7 MHz, $CDCl_3$): δ 7.46–7.45 (m, 4H, Ph), 7.41 – 7.39 (m, 1H, Ph), 7.06 (d, 1H, $^3J_{H,H}$ = 2.0 Hz, CH_{im}), 6.72 (d, 1H, $^3J_{H,H}$ = 2.0 Hz, CH_{im}), 6.41 (d, 1H, $^2J_{H,H}$ = 15.1 Hz, CH_2Ph), 6.27 (d, 1H, $^2J_{H,H}$ = 15.1 Hz, CH_2Ph), 4.84 (m, 1H, NBD), 4.70 (m, 1H, NBD), 3.81 (br s, 1H, NBD), 3.78 (br s, 1H, NBD), 3.47 (m, 2H, NBD), 2.08 (s, 9H, ^{t}Bu), 1.36 (d, 1H, $^2J_{H,H}$ = 8.0 Hz, NBD), 1.31 (d, 1H, $^2J_{H,H}$ = 8.0 Hz, NBD). ^{13}C NMR (150.8 MHz, $CDCl_3$): δ 183.0 (d, $J_{C,Rh}$ = 58.5 Hz), 136.9 (C_q, Ph), 128.7 (Ph), 128.0 (Ph), 127.8 (Ph), 119.7 (CH_{im}), 119.6 (CH_{im}), 74.9 (d, $J_{C,Rh}$ = 6.1 Hz, NBD), 71.8 (d, $J_{C,Rh}$ = 6.3 Hz, NBD), 62.7 (d, $J_{C,Rh}$ = 5.2 Hz, NBD), 57.9 (C_q, ^{t}Bu), 56.3 (CH_2Ph), 48.2 (d, $J_{C,Rh}$ = 12.7 Hz, NBD), 46.3 (d, $J_{C,Rh}$ = 12.1 Hz, NBD), 32.1 (^{t}Bu). ESI-MS (MeOH, *m/z*): 409 (100) $[M - Cl]^+$. Anal. Calcd (%) for $C_{21}H_{26}ClN_2Rh$: C, 56.70; H, 5.89; N, 6.30. Found: C, 56.51; H, 5.87; N, 6.41.

4.2.7 [RhCl(NBD){1-butyl-3-methyl-imidazolin-2-ylidene}] (5). To a solution of 1-butyl-3-methylimidazolium bromide (0.10 g, 0.46 mmol) in CH_2Cl_2 (10 mL), Ag_2O (0.058 g, 0.25 mmol) was added. The suspension was stirred for 48 h then, solid $[Rh(NBD)Cl]_2$ (0.10 g, 0.22 mmol) was directly added to the reaction mixture. After stirring for further 24 h the crude material was filtered on a celite pad, the insoluble material was thoroughly washed with CH_2Cl_2 and the solvent removed under vacuum. The residue was purified by column chromatography on silica gel using Et_2O:CH_2Cl_2 1:1 (v/v) to afford **5** as a yellow solid (0.13 g, 80 %). R_f: 0.68 (CH_2Cl_2:MeOH 100:5). ^{1}H NMR (300.1 MHz, $CDCl_3$): δ 6.76 (d, 1H, $^3J_{H,H}$ = 1.7 Hz, CH_{im}), 6.75 (d, 1H, $^3J_{H,H}$ = 1.7 Hz, CH_{im}), 4.84 (s, 2H, NBD), 4.47 (t, 2H, $^3J_{H,H}$ = 7.5 Hz, NCH_2), 4.07 (s, 3H, NCH_3) 3.93 (br s, 2H, NBD), 3.47 (br s, 2H, NBD), 1.91 (m, 2H, CH_2), 1.35 (m, 2H, CH_2), 1.20 (s, 2H, NBD), 1.05 (t, 3H, $^3J_{H,H}$ = 7.2 Hz, CH_3). ^{13}C NMR (75.5 MHz, $CDCl_3$): δ 181.7 (d, $J_{C\text{-}Rh}$= 57.5 Hz), 120.9 (CH_{im}), 119.2 (CH_{im}), 77.1 (d, $J_{C\text{-}Rh}$ = 6.0 Hz, NBD), 62.8 (d, $J_{C\text{-}Rh}$ = 5.1 Hz, NBD), 50.1 (NBD), 49.3 (NCH_2), 36.7 (NCH_3), 32.4 (CH_2), 19.0 (CH_2), 12.8 (CH_3). Anal. Calcd (%) for $C_{15}H_{22}ClN_2Rh$: C, 48.86; H, 6.01; N, 7.60. Found: C, 48.97; H, 5.93; N, 7.63.

4.3 X-ray structure determination for 2b, 3a and 3b. Crystal data were collected at room temperature on a Bruker APEX II diffractometer equipped with a CCD detector operating at 50 kV and 30 mA, using graphite-monochromated Mo Kα radiation (λ = 0.71073 Å). An empirical absorption correction was applied on both structures by using SADABS.[33] They were solved by direct methods and refined by full-matrix least-squares based on all data using F^2 with SHELXL97.[34] All non-hydrogen atoms were refined anisotropically, with the exception of the hydrogen atoms, which were set geometrically and given fixed isotropic thermal parameters. Crystal data are collected in Table 3S.

4.4 Variable Temperature NMR. VT spectra were recorded using spectrometers at 400 and 600 MHz for ^{1}H. The NMR tubes containing the compounds were prepared under an argon atmosphere using a vacuum line. Low-temperature ^{1}H spectra were acquired without spinning using a 5 mm dual direct probe with a 6000 Hz (at 400 MHz) or 9000 Hz (at 600 MHz) sweep width, 40° tip angle pulse width, 3 s acquisition time, and 1 s delay time. A shifted sine bell weighting function equal to the acquisition time (i.e., 3 s) was applied before the Fourier transformation. Usually 32 to 64 scans were collected. When operating the NMR apparatus at low temperature, a flow of dry nitrogen was first passed through a precooling unit adjusted to -50°C. Then the gas entered into an inox steel heat-exchanger immersed in liquid nitrogen and connected to the NMR probe head by a vacuum-insulated transfer line. Gas flows of 10 to 20 L min^{-1} were required to reach the desired temperature. Temperature calibrations were performed before the experiments, using a digital thermometer and a Cu/Ni thermocouple placed in an NMR tube filled with isopentane for the low-temperature range and with 1,1,2,2-tetrachloroethane for the high-temperature range. The conditions were kept as identical as possible with all subsequent work. In particular, the sample was not spun and the gas flow was the same as that used during the acquisition of the spectra. The uncertainty in temperature measurements can be estimated from the calibration curve as ±2 °C. Line shape simulations were performed using a PC version of the QCPE DNMR6 program.[35] Electronic

superimposition of the original spectrum and of the simulated one enabled the determination of the most reliable rate constant. The rate constants, thus obtained at various temperatures, afforded the free energy of activation $\Delta G^{\ddagger}$ by applying the Eyring equation. $\Delta H^{\ddagger}$ and $\Delta S^{\ddagger}$ were evaluated by linear regression of the $\Delta G^{\ddagger}$ value vs the temperature. Except for **3c**, in all cases investigated, the activation energy $\Delta G^{\ddagger}$ was found to be virtually invariant in the given temperature range, thus implying a very small or negligible activation entropy $\Delta S^{\ddagger}$. 1D-EXSY spectra were acquired using the standard DPFGSE-NOE sequence, using arrayed mixing times (25,50,75 and 100 ms).

4.5 DFT Calculations. Conformational searches were performed by Molecular Mechanics (MMFF force field as implemented in Titan 1.0.5, Wavefunction inc.). Final geometry optimizations were carried out at the B3LYP/LANL2DZ level[36] by means of the Gaussian 09 series of programs[37] (see the Supporting Information). The standard Berny algorithm in redundant internal coordinates and default criteria of convergence were employed in all the calculations. Harmonic vibrational frequencies were calculated for all the stationary points. For each optimized ground state the frequency analysis showed the absence of imaginary frequencies, whereas each transition state showed a single imaginary frequency. Visual inspection of the corresponding normal mode was used to confirm that the correct transition state had been found. All the reported energy values represent total electronic energies. In general, these give the best fit with experimental DNMR data.[38] Therefore, the computed numbers have not been corrected for zero-point energy contributions or other thermodynamic parameters. This avoids artefacts that might result from the ambiguous choice of the adequate reference temperature, from the empirical scaling[39] and from the treatment of low-frequency vibration as harmonic oscillators.[40]

4.6 Catalysis

General procedure for the hydrosilylation of 1-alkynes with $HSiMe_2Ph$

In a typical experiment a J.Young valve NMR tube was charged under argon with the catalyst precursor **3a**, **3d** or **5** ($7.7x10^{-4}$ mmol or $7.7x10^{-5}$ mmol), $CDCl_3$ (0.6 mL), the corresponding alkyne (0.077 mmol), and a slight excess of $HSiMe_2Ph$ (0.085 mmol). The solution was kept at T = 25°C or at 60 °C and monitored by ^{1}H-NMR spectroscopy. The products were unambiguously characterized by ^{1}H NMR spectroscopy by comparison with literature spectra,[2] further details on the NMR spectra and integrations are reported in the Supporting Information.

Supporting Information

Electronic Supplementary Information (ESI) available: additional experimental and characterization data; crystal data and experimental details for all structures, molecular structure of **2b**; computational details; additional graphs and experimental data for the catalysis. X-ray data in the form of CIF files for **2b**, **3a** and **3b**. CCDC 957761 for compound **3a** and 957762 for **3b**.

Acknowledgment

The authors wish to thank the University of Bologna and the Ministero dell'Università e della Ricerca (MUR) (project: "New strategies for the control of reactions: interactions of molecular fragments with metallic sites in unconventional species", PRIN 2009) for financial support. We also thank Dr. R. Cirilli (Istituto Superiore di Sanità, Department of Therapeutic Research and Medicines Evaluation, Rome) for HPLC analyses.

References

1 For reviews on N-heterocyclic carbenes see: (a) L. A. Schaper, S. J. Hock, W. A. Herrmann and F. E. Kühn, *Angew. Chem. Int. Ed.,* 2013, **52**, 270; (b) L. Benhamou, E. Chardon, G. Lavigne, S. Bellemin-Laponnaz and V. César, *Chem. Rev.,* 2011, **111**, 2705; (c) L. Mercs and M. Albrecht, *Chem. Soc. Rev.,* 2010, **39**, 1903; (d) S. Diez-Gonzalez, N. Marion and S. P. Nolan, *Chem. Rev.,* 2009, **109**, 3612; (e) H. Jacobsen, A. Correa, A. Poater, C. Costabile and L. Cavallo, *Coord. Chem.*

Rev., 2009, **253**, 687; (f) F. E. Hahn, ed. of themed issue: N-Heterocyclic carbenes, *Dalton Trans.,* 2009, **35**, 6873; (g) F. E. Hahn and M. C. Jahnke, *Angew. Chem. Int. Ed.,* 2008, **47**, 3128; (h) R. H. Crabtree, *Coord. Chem. Rev.,* 2007, **251**, 595 ff.: a volume completely dedicated to recent developments in the organometallic chemistry of N-heterocyclic carbenes; (i) C. M. Crudden and D. P. Allen, *Coord. Chem. Rev.,* 2004, **248**, 2247; (j) W. A. Herrmann, *Angew. Chem. Int. Ed.,* 2002, **41**, 1290; (k) D. Bourissou, O. Guerret, F. P. Gabbai and G. Bertrand, *Chem. Rev.,* 2000, **100**, 39.

2 L. Busetto, M. C. Cassani, C. Femoni, M. Mancinelli, A. Mazzanti, R. Mazzoni and G. Solinas, *Organometallics,* 2011, **30**, 5258.

3 For recent reports on Rh(I)(NHC) catalysed hydrosilylation and hydrothiolation see: (a) M. V. Jimenez, J. J. Perez-Torrente, M. I. Bartolomè, V. Gierz, F. J. Lahoz, and L. A. Oro, *Organometallics,* 2008, **27**, 224; (b) B. J. Truscott, A. M. Z. Slawin and S. P. Nolan, *Dalton Trans.,* 2013, **42**, 270; (c) A. Monney, F. Nastri, M. Albrecht, *Dalton Trans.*, 2013, **42**, 5655; (d) M. Steinbeck, G. D. Frey, W. W. Schoeller and W. A. Herrmann, *J. Organomet. Chem.,* 2011, **696**, 3945; (e) J. J. Dunsford, D. S. Tromp, K. J. Cavell, C. J. Elsevier, B. M. Kariuki, *Dalton Trans.,* 2013, **42**, 7318; (f) A. Di Giuseppe, R. Castarlenas, J. J. Pérez-Torrente, M. Crucianelli, V. Polo, R. Sancho, F. J. Lahoz and L. A. Oro, *J. Am. Chem. Soc*., 2012, **134**, 8171.

4 S. Patil, A. Deally, B. Gleeson, M. Helge, F. Paradisi, M. Tacke, *Appl. Organometal. Chem*., 2010, **24**, 781.

5 S. Patil, J. Claffey, A. Deally, M. Hogan, B. Gleeson, L. M. Menéndez Méndez, H. Müller-Bunz, F. Paradisi and M. Tacke, *Eur. J. Inorg. Chem.,* 2010, 1020.

6 In case of **1d** the alkylation of 1-benzylimidazole with 1-*tert*-butyl bromide does not afford the desired product due to the occurrence of an elimination reaction, in which the *tert*-butyl bromide in the presence of 1-benzylimidazole releases a molecule of HBr (with evolution of isobutene gas) which further reacts with benzylimidazole to form the corresponding imidazolium bromide salt. See: R. Corberán, M. Sanaú, E. Peris, *Organometallics,* 2006, **25**, 4002.

7 C. Hirtenlehner, C. Krims, J. Hölbling, M. List, M. Zabel, M. Fleck, R. J. F. Berger, W. Schoefberger, U. Monkowius, *Dalton Trans.,* 2011, **40**, 9899.

8 The silver complex **2b** has been also characterized by X-ray diffraction (see Table 3S and Fig. 2S) and the structural data are in perfect agreement (within the experimental error) with those reported in C. P. Newman, G. J. Clarkson and J. P. Rourke, *J. Organomet. Chem*., 2007, **692**, 4962.

9 S. Ray, R. Mohan, J. K. Singh, M. K. Samantaray, M. M. Shaikh, D. Panda and P. Ghosh, *J. Am. Chem. Soc*., 2007, **129**, 15042.

10 (a) J. C. Garrison and W. J. Youngs, *Chem. Rev.*, 2005, **105**, 3978; (b) P. de Frémont, N. M. Scott, E. D. Stevens, T. Ramnial, O. C. Lightbody, C. L. B. Macdonald, J. A. C. Clyburne, C. D. Abernethy and S. P. Nolan, *Organometallics,* 2005, **24**, 6301.

11 J. Li, J. Peng, Y. Bai, G. Lai and X. Li, *J. Organomet. Chem.*, 2011, **696**, 2116.

12 A. Bittermann, P. Härter, E. Herdtweck, S. D. Hoffmann and W. A. Herrmann, *J. Organomet. Chem*., 2008, **693**, 2079.

13 For a review see: D. Casarini, L. Lunazzi and A. Mazzanti, *Eur. J. Org. Chem*., 2010, 2035.

14 Due the identity of the two substituents, compound **3b** actually belongs to the C_s symmetry.

15 Despite the C_s symmetry of **3b**, the NMR signal of the CH_2 is still a stereochemical probe because the local plane of symmetry does not correspond to the symmetry plane of the molecule. See W. B. Jennings, *Chem. Rev.,* 1975, **75**, 307.

16 (a) D. Enders, H. Gielen, J. Runsink, K. Breuer, S. Brode and K. Boehn, *Eur. J. Inorg. Chem.,* 1998, 913; (b) D. Enders and H. Gielen, *J. Organomet. Chem.*, 2001, **617**, 70.

17 The 1D EXSY experiment was acquired using the standard DPFGSE-NOE sequence with short mixing times; (a) L. Lunazzi, M. Mancinelli, A. Mazzanti and M. Pierini, *J. Org. Chem*., 2010, **75**, 5927; (b) L. Lunazzi, M. Mancinelli and A. Mazzanti, *J. Org. Chem.,* 2012, **77**, 3373.

18 L. Lunazzi, G. Panciera and M. Guerra, *J. Chem. Soc. Perkin Trans.,* 1980, **2**, 52.

19 H. Iwamura and K. Mislow, *Acc. Chem. Res.* 1988, **21**, 175.

20 C. Boga, E. Del Vecchio, L. Forlani, A. Mozzanti and P. E. Todesco, *Angew. Chem. Int. Ed.,* 2005, **44**, 3285.

21 H. Hedayat, A. Naader, S. Mojtaba and A. Zouhair, *J. Phys. Chem. A,* 2010, **114**, 7462.

22 (a) C. Wolf, *Chem. Soc. Rev.,* 2005, **34**, 595; (b) I. D'Acquarica, F. Gasparrini, M. Pierini, C. Villani and G. Zappia, *J. Sep. Sci.,* 2006, **29**, 1508; (c) F. Piron, N. Vanthuyne, B. Joulin, J.-V. Naubron, C. Cismas, A. Terec, R. A.Varga, C. Roussel, J. Roncali and I. Grosu, *J. Org. Chem.*, 2009, **74**, 9062.

23 W. Gil, T. Lis, A. M. Trzeciak and J. J. Ziołkowski, *Inorg. Chim. Acta*, 2006, **359**, 2835.

24 TOF calculated for a reaction time of 2 h which corresponds for complex **5** to a conversion of 54%.

25 (a) A. T. Normand, K. J. Cavell, *Eur. J. Inorg. Chem.*, 2008, 2781; (b) O. Kühl, *Chem. Soc. Rev.*, 2007, **36**, 592; (c) D. Pugh and A. A. Danopoulos, *Coord. Chem. Rev.*, 2007, **251**, 610; (d) S. T. Liddle, I. S. Edworthy and P. L. Arnold*, Chem. Soc. Rev.,* 2007, **36**, 1732; (e) P. L. Arnold, S. A. Mungur, A. J. Blake and C. Wilson, *Angew. Chem. Int. Ed*., 2003, **42**, 5981. (f) W. A. Herrmann, C. Köcher, L. J. Gooßen and G. R. J. Artus, *Chem. Eur. J.*, 1996, **2**, 1627; (g) H. Ohara, W. N. O. Wylie, A. J. Lough and R. H. Morris, *Dalton Trans.*, 2012, **41**, 8797.

26 (a) M. Poyatos, E. Mas-Marzà, J. A. Mata, M. Sanau and E. Peris, *Eur. J. Inorg, Chem.* 2003, 1215; (b) I. Ojima, N. Clos, R. J. Donovan and P. Ingallina, *Organometallics*, 1990, **9**, 3127.

27 G. de Bo, G. Berthoz-Gelloz, B. Tinant and I. E. Markò, *Organometallics*, 2006, **25**, 1881.

28 A. K. Roy, *Adv. Organomet. Chem.* 2008, **55**, 1 and references therein.

29 Z. T. Ball, *Comprehensive Organometallic Chemistry III, Vol. 10:Application II: Transition metal Compounds in Organic synthesis 1*, R. H. Crabtree, M. Mingos Eds., Elsevier: Oxford, 3rd edn., 2006, 789-813.

30 C. H. Jun and R. H. Crabtree, *J. Organomet. Chem.*, 1993, **447**, 177.

31 S. Sauerbrey, P. K. Majhi, J. Daniels, G. Schnakenburg, G. M. Brändle, K. Scherer and R. Streubel, *Inorg. Chem.,* 2011, **50**, 793.

32 D. D. Perrin, W. L. F. Armarego and D. R. Perrin, *Purification of Laboratory Chemicals,* Pergamon Press: New York, 2nd edn., 1980.

33 G. M. Sheldrick, SADABS, University of Gottingen, Germany, 1996.

34 G. M. Sheldrick, SHELXL97, University of Gottingen, Germany.

35 The program is available from the authors on request.

36 For B3LYP functional: (a) A. D. Becke, *J. Chem. Phys.*, 1993, **98**, 5648; (b) C. Lee, W. Yang and R. G. Parr, *Phys. Rev. B,* 1988, **37**, 785; (c) P. J. Stephens, F. J. Devlin, C. F. Chabalowski and M. J. Frisch, *J. Phys. Chem.,* 1994, **98**, 11623. For the LanL2DZ basis set: P. J. Hay and W. R. Wadt, *J. Chem. Phys.,* 1985, **82**, 299.

37 Gaussian 09 rev A.02. M. J. Frisch, G. W. Trucks, H. B. Schlegel, G. E. Scuseria, M. A. Robb, J. R. Cheeseman, G. Scalmani, V. Barone, B. Mennucci, G. A. Petersson, H. Nakatsuji, M. Caricato, X. Li, H. P. Hratchian, A. F. Izmaylov, J. Bloino, G. Zheng, J. L. Sonnenberg, M. Hada, M. Ehara, K. Toyota, R. Fukuda, J. Hasegawa, M. Ishida, T. Nakajima, Y. Honda, O. Kitao, H. Nakai, T. Vreven, J. A. Montgomery, Jr., J. E. Peralta, F. Ogliaro, M. Bearpark, J. J. Heyd, E. Brothers, K. N. Kudin, V. N. Staroverov, R. Kobayashi, J. Normand, K. Raghavachari, A. Rendell, J. C. Burant, S. S. Iyengar, J. Tomasi, M. Cossi, N. Rega, N. J. Millam, M. Klene, J. E. Knox, J. B. Cross, V. Bakken, C. Adamo, J. Jaramillo, R. Gomperts, R. E. Stratmann, O. Yazyev, A. J. Austin, R. Cammi, C. Pomelli, J. W. Ochterski, R. L. Martin, K. Morokuma, V. G. Zakrzewski, G. A. Voth, P. Salvador, J. J. Dannenberg, S. Dapprich, A. D. Daniels, Ö. Farkas, J. B. Foresman, J. V. Ortiz, J. Cioslowski and D. J. Fox, Gaussian, Inc., Wallingford CT, 2009.

38 P. Y. Ayala and H. B. Schlegel, *J. Chem. Phys.*, 1998, **108**, 2314.

39 C. F. Tormena, R. Rittner, R. J. Abraham, E. A. Basso and B. C. Fiorin, *J. Phys. Org. Chem.*, 2004, **17**, 42.

40 (a) M. W. Wong, *Chem. Phys. Lett.*, 1996, **256**, 391; (b) S. E. Wheeler, A. J. McNeil, P. Müller, T. M. Swager and K. N. Houk, *J. Am. Chem. Soc.*, 2010, **132**, 3304.